Pergamon

Acta Materialia 50 (2002) 2779–2786

Acta MATERIALIA

www.actamat-journals.com

Effect of native Al_2O_3 on the elastic response of nanoscale Al films

M.T.A. Saif [a,*], S. Zhang [b], A. Haque [a], K.J. Hsia [b]

[a] *Mechanical and Industrial Engineering, University of Illinois at Urbana-Champaign, Urbana, IL 61801, USA*
[b] *Theoretical and Applied Mechanics, University of Illinois at Urbana-Champaign, Urbana, IL 61801, USA*

Received 23 December 2001; received in revised form 20 February 2002; accepted 20 February 2002

Abstract

A continuous, dense aluminum oxide (Al_2O_3) layer of about 5 *nm* forms on the surface of Al upon exposure to oxygen or dry air. Since the elastic moduli of Al and Al_2O_3 are 69 *GPa* and 370 *GPa*, respectively, the elastic modulus of a thin Al film of sub-micron dimension (with the native oxide layer) should be much higher than that of pure Al. However, uniaxial tensile measurements on Al films with thickness down to 50 *nm* revealed an effective modulus close to 69 *GPa*. In the present paper, we investigate a plausible mechanism for this discrepancy, namely, the effect of *wavy surface* oxide layer. Here thin Al films are considered as Al-Al_2O_3 composites. Uniaxial tensile experiments on a free-standing, 200 *nm* thick Al film are performed using MEMS techniques. The surface morphology of the specimen is characterized by AFM. An analytical model is developed to estimate the effective modulus, $\bar{E}$, of a wavy oxide layer. The current study shows that the model predictions using measured material parameters agree reasonably well with the experimental results, thus supporting the validity of the proposed mechanism.

1. Introduction

Aluminum, upon exposure to oxygen or dry air at room temperature, forms a thin layer of amorphous native Al_2O_3. The thickness of Al_2O_3 becomes 2~4 *nm* in several hours, and reaches a value of about 5 *nm* after a long time [1]. Since the molar volume of Al_2O_3 is 1.7 times that of Al, the oxide forms a continuous film [1,2,3] on the Al surface, offering a natural sealant against corrosion of the substrate.

Although the effect of the native oxide layer on the elastic modulus of Al is negligible for bulk components, its role becomes important for thin Al films of sub-micron dimension, typical in micro electronic and micro-electro-mechanical-system (MEMS) applications [4]. Considering that the elastic moduli of Al_2O_3 and polycrystalline Al are 370 *GPa* and 69 *GPa*, respectively [5], the Al-Al_2O_3 composite thin film is expected to have an in-plane effective modulus higher than that of pure Al, given by the simple rule of mixture, as

$$E_{\text{comp}} = E_{\text{Al}} t_{\text{Al}}/t_{\text{tot}} + E_{\text{ox}} t_{\text{ox}}/t_{\text{tot}} \quad (1)$$

* Corresponding author. Tel.: +1 217 333 8552; fax: +1 217 244 655.
E-mail address: saif@uiuc.edu (M.T.A. Saif).

1359-6454/02/$22.00
PII: S1359-6454(02)00089-7

where E_{comp}, E_{Al}, and E_{ox} denote the moduli of the composite, Al film, and oxide layer, respectively, and t_{tot}, t_{Al} and t_{ox} are the thicknesses of Al film, oxide layer (both sides of the film), and composite, respectively (Fig. 1c).

Mearini and Hoffman [3] carried out uniaxial tests on Al thin films of 50~160 *nm* in thickness, covered with a native oxide layer. Contrary to the prediction by Eq. (1), they found the composite Young's modulus to be close to that of pure Al. They speculated that the native oxide layer might be porous, similar to anodized Al_2O_3, or that the oxide might form cracks during straining, thus resulting in its lower elastic modulus of about 100 *GPa*. These conjectures, however, were not supported by experimental evidence. In fact, even if $E_{ox} \approx 100$ *GPa*, the composite modulus is expected to increase monotonically as composite thickness decreases. No such trend was observed in the measurements by Mearini and Hoffman [3] when the thickness of Al was reduced from 160 to 50 *nm*. Uniaxial tension experiments on free standing Al films were also carried out by Huang and Spaepen [6], and the elastic modulus was found to be lower than that of bulk Al.

In the present paper, we verify the results of Mearini and Hoffmann [3] by carrying out a uniaxial tensile experiment on a free-standing, 200 *nm* thick sputtered Al film with native oxide. Our results confirm that the composite elastic modulus is lower than that given by Eq. (1). A plausible mechanism, the effect of surface waviness of the native oxide layer, induced by the roughness of a sputtered Al surface, is investigated. We develop a simple model based on curved beam theory to estimate the effective modulus of the oxide layer.

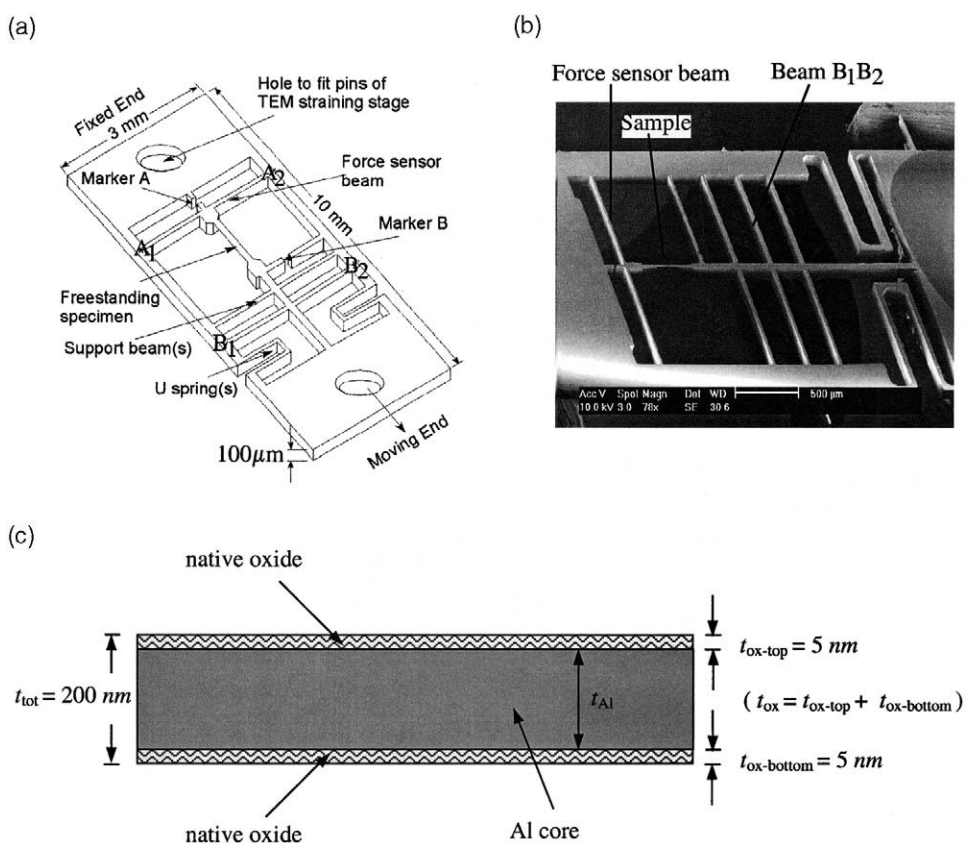

Fig. 1. (a) Schematic of the loading stage. (b) Scanning electron micrograph of the loading stage with the sample. (c) Cross section (schematic) of the sample.

Using our surface roughness measurements by an atomic force microscope (AFM) and our model, we have obtained an estimate of the effective modulus of the composite film, which agrees with the measured value.

2. Uniaxial tension experiment on a free-standing Al film

The experimental setup (Fig. 1) consists of a free-standing thin Al specimen and a loading stage made from single crystal silicon. The sample is 200 *nm* thick, 23.5 μm wide, and 185 μm long made from sputtered Al. One end of the sample is attached to the middle of a silicon flexural beam, A_1A_2, with a known lateral spring constant, *c*, calibrated by a nano-indenter after the tensile experiment. A_1A_2 serves as a force sensor. The other end of the specimen is attached to a set of parallel beams, B_1B_2. Axial loading is applied by controlled displacement at one end of the stage by a piezo actuator, while holding the other end fixed. The load, *F*, on the sample is measured from $F=c\delta$, where δ is the mid displacement of A_1A_2, and is measured from marker A when the experiment is carried out in-situ in a scanning electron microscope (SEM). The axial strain in the specimen is determined from the relative displacements between markers A and B.

A critical concern in a uniaxial tension experiment is the alignment between the specimen and loading direction. A slight misalignment may cause sufficient unaccounted non-uniformity of stress across the sample cross-section giving an apparent lower elastic constant. Here, the alignment is ensured by (1) lithographic patterning and co-fabrication of the sample and the stage which avoid any assembly; and (2) designing the set of beams B_1B_2 and the flexure structures around them such that a misalignment error is reduced by five orders of magnitude. The details of fabrication of the sample and the loading fixture, as well as an analysis on alignment are provided in [7].

Fig. 2 shows the linear stress–strain behavior of the specimen with yielding at 350 *MPa*, and an elastic modulus of 74.6 *Gpa* obtained from the best-fit line. However, Eq. (1) predicts an elastic

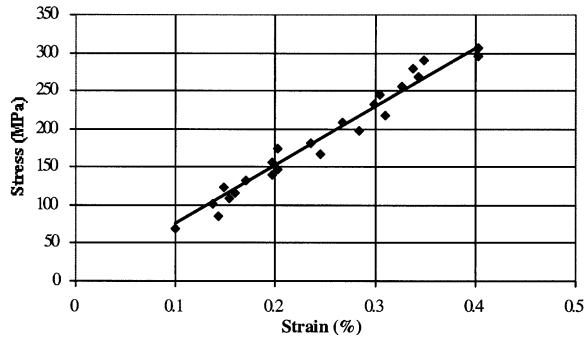

Fig. 2. Stress strain response of the 200 *nm* thick Al film under uniaxial loading. Yielding occurs at around 350 *MPa*.

modulus of the specimen (t_{Al}=190 *nm*, t_{ox}=10 *nm*) of E_{comp}=85 *GPa*, 14% higher than the measured result. Similar discrepancy is reported by Mearini and Hoffman [3]. Note that the high yield stress (350 *MPa*) is typical of small grain (100 *nm* for our specimen as measured by TEM) Al film. A uniaxial experiment on a 100 *nm* thick Al film using a similar MEMS force sensor was carried out by Haque and Saif [8], and the elastic modulus was found to be 69.6 *GPa*. Thus the stiffening effect of the oxide coating was not observed.

3. The mechanism: surface waviness

We believe that the mechanism responsible for such discrepancy is not the porosity but the waviness of the native oxide surface. Since the native oxide layer grows uniformly from the Al substrate when the Al thin film is exposed to air, any roughness on the Al surface will be faithfully duplicated. This will result in a continuous oxide layer with uniform thickness of about 5 *nm*, and the same surface morphology as the Al film underneath. Such oxide layer, with sufficient roughness, will be significantly more flexible when loaded along the nominal surface plane because, in addition to the in-plane stretching, there will be bending of the layer due to surface waviness.

To study this mechanism, we measured the waviness of both the top and the bottom surfaces of the Al film using an AFM. Fig. 3a shows a typical surface morphology of a 3 $\mu m \times 3$ μm region from the top surface of the Al film. It clearly demon-

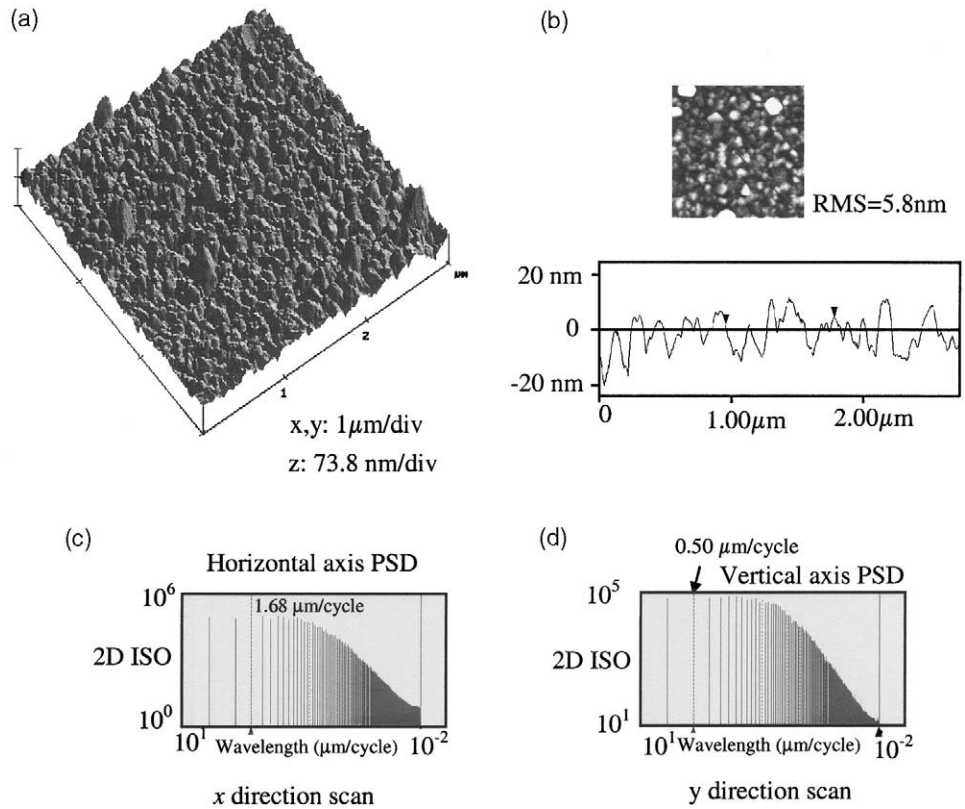

Fig. 3. Atomic Force Microscope measurements of the top surface of the Al film used in the uniaxial experiment. (a) A 3-D image of the surface; (b) topography of the surface; (c) a line scan of the surface; and (d) power spectral density of surface roughness when scanned along *x* and *y* directions.

strates that the oxide layer surface is indeed wavy. Fig. 3b shows the topography with color contrast. Fig. 3c shows the profile of a line scan between two points on the surface. Fig. 3d shows the power spectral density (PSD) of the topography when scanned along *x* and *y* directions. These figures show that the amplitude of the waviness varies within 0~20 *nm* from the nominal surface plane with root mean square (RMS) value of 6 *nm*. The RMS value for the bottom surface is 3.5 *nm*. The lower roughness of the bottom surface is most likely due to the sputter deposition of the Al film on a smooth silicon surface. The effect of such wavy surface is analyzed in the following using a simple model.

4. Analytical model: effective Young's modulus of a wavy oxide beam

To analyze the effect of wavy oxide surface layer, we consider the oxide layer alone, and approximate the two dimensional wavy surface by a wavy beam. The effective Young's modulus of the wavy beam can be obtained by analyzing its stress–strain response upon loading along the nominal longitudinal axis of the beam.

For a wavy beam of nominal length s_0, subjected to a tensile load, P, at the ends, the total end displacement, Δ, can be determined by using the Principle of Virtual Work (see, e.g., [9])

$$\Delta = \int_0^{s_0} \frac{N_u N_L}{EA} ds + \int_0^{s_0} \frac{M_u M_L}{EI} ds + \int_0^{s_0} \frac{\alpha_s Q_u Q_L}{GA} ds \qquad (2)$$

where N_u, M_u and Q_u are the axial force, bending moment and shear force on the beam, respectively, caused by a unit tensile load P_u=1 at the ends of the beam, N_L, M_L and Q_L are the tension, bending moment and shear, respectively, caused by the applied tensile force P, α_s is the shear coefficient, A and I are the area and moment of inertia of the cross section, respectively, and E and G are tensile and shear modulus, respectively.

The deformation of a wavy beam of uniform thickness t with random surface waviness, such as that shown in the line scan of Fig. 3(c), can be analyzed by considering individual unit cells, depicted in Fig. 4(a). The shape of each unit cell can be described by a function, $y=f(x)$. The important parameters characterizing the shape of a unit cell are h, the wave amplitude, and d, the wavelength, as seen in Fig. 4(b). By superposition, the overall stretch of a wavy beam caused by force P can be evaluated.

For a unit cell with dimensions given in Fig. 4(b) under external force P, the force components in the beam are

$$N_L = P\cos\theta,\ Q_L = P\sin\theta,\ \ M_L = Pf(x) \tag{3a}$$

and

$$N_u = \cos\theta,\ Q_u = \sin\theta,\ \ M_u = f(x) \tag{3b}$$

where θ is the tangential angle of the beam with respect to the loading direction. The end displacement caused by the tension, shear and bending moment, denoted by Δ^T, Δ^S, Δ^M, respectively, can be expressed as

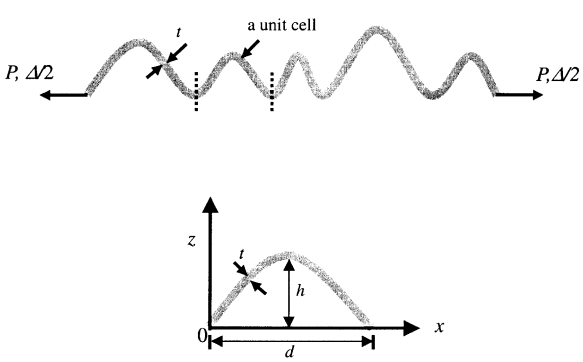

Fig. 4. (a) Schematic representation of the oxide coating on Al as a wavy beam. (b) a unit cell representing a segment of the wavy beam.

$$\Delta^T = \frac{P}{EA}\int_0^d \cos\theta dx, \Delta^S = \frac{\alpha_S P}{GA}\int_0^d \frac{\sin^2\theta}{\cos\theta}dx, \tag{4}$$

$$\Delta^M = \frac{P}{EI}\int_0^d \frac{f^2(x)}{\cos\theta}dx$$

Thus, the overall stretch of the unit cell is

$$\Delta = \Delta^T + \Delta^S + \Delta^M \tag{5}$$

The effective Young's modulus of the unit cell can be given as

$$\bar{E} = \frac{\sigma}{\varepsilon} = \frac{Pd}{A\Delta} \tag{6}$$

To simplify the analysis, we consider a sinusoidal form for the shape of the unit cell, as

$$y = f(x) = h\sin(\pi x/d) \tag{7}$$

Substituting (7) into (4), we have

$$\Delta^T = \frac{Pd}{EA}F^T, \Delta^S = \frac{\alpha_S Pd}{GA}F^S, \Delta^M = \frac{Pd}{EI}F^M \tag{8}$$

where

$$F^T = \frac{2}{\pi}\sqrt{1-k^2}K_1(k) \tag{9a}$$

$$F^S = \frac{2}{\pi}\left[\frac{K_2(k)}{\sqrt{1-k^2}} - \sqrt{1-k^2}K_1(k)\right] \tag{9b}$$

$$F^M = \frac{2}{3\pi^2\sqrt{1-k^2}}[(h^2\pi^2-d^2)K_2(k) + d^2K_1(k)] \tag{9c}$$

and $k^2 = h^2\pi^2/(h^2\pi^2 + d^2)$, $K_1(k)$ and $K_2(k)$ are the first and second complete elliptical integrals defined, respectively, as $K_1(k) = \int_0^{\pi/2} \frac{d\psi}{\sqrt{1-k^2\sin^2\psi}}$ and $K_2(k) = \int_0^{\pi/2} \sqrt{1-k^2\sin^2\psi}d\psi$. Noting that $I = At^2/12$, $G = E/2(1+\nu)$, and $\alpha_s = (7+$

$6\nu)/6(1+\nu)$, the end displacement of the unit cell under the axial loading P is

$$\Delta = \Delta^{T} + \Delta^{S} + \Delta^{M} = \frac{Pd}{EA}F \tag{10}$$

where

$$F = F^{T} + 2\alpha_{S}(1+\nu)F^{S} + 12F^{M}/t^{2} \tag{11}$$

is a function dependent on the shape of the unit cell. The effective Young's modulus, $\bar{E}$, of the unit cell is given by

$$\bar{E} = \frac{P/A}{\Delta/d} = \frac{E}{F} \tag{12}$$

Fig. 5 shows the dependence of the effective Young's modulus, $\bar{E}$, normalized by the intrinsic Young's modulus, E, on the parameters d/t and h/t for a beam with periodic wavy shape given by Eq. (7). Here ν=0.22 is used. The plot shows that the effective Young's modulus drops dramatically as the normalized wave amplitude h/t increases. However, the effective Young's modulus does not change significantly as the wavelength d/t varies from 1–5. As an example, for d/t=2.0 and h/t=1.0, Eq. (12) predicts $\bar{E}/E = 0.097$; with E_{ox}=370 *GPa*, $\bar{E} = 35.9GPa$.

5. Stochastic modeling of surface roughness

The real surface roughness, off course, may not be approximated by a simple sinusoidal wave. Statistical variations of the surface waviness must be taken into account in order to compare our model prediction with our experimental measurements. Our objective is to estimate an average or a mean value of $\bar{E}$ of the oxide coating, taking account of the surface roughness as follows.

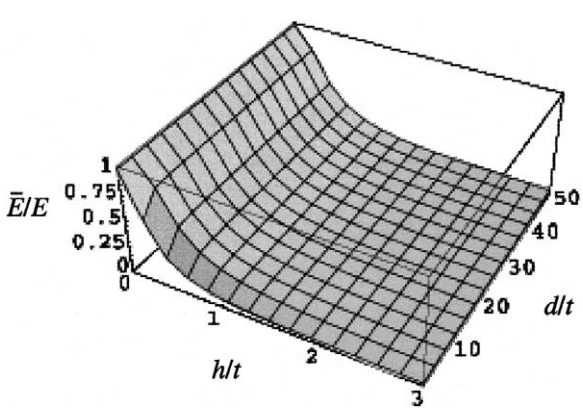

Fig. 5. Normalized effective Young's modulus of a sinusoidal beam as a function of the shape parameters h/t and d/t.

Since the oxide layer is bonded to the Al substrate, we assume that, under uniaxial tension at low stress, no debonding occurs. Then, it is reasonable to assume that during the experiment, the nominal in-plane strain of the oxide layer is the same as the in-plane strain, ε, of the Al substrate. In other words, if the distance (along the loading direction) between any two points on the oxide film is X before loading, then their distance (along the loading direction) after loading is $X(1+\varepsilon)$. These points can be at any elevation of the rough surface. The effective modulus, $\bar{E}$, of the oxide film varies from point to point depending on the amplitude of roughness in the vicinity of the point. Thus, for a uniform strain, ε, the nominal in-plane stress of oxide also varies statistically. In order to estimate an expected value of $\bar{E}$, consider a long longitudinal strip of a planar film, shown in Fig. 6, which represents the wavy oxide film without the Al sub-

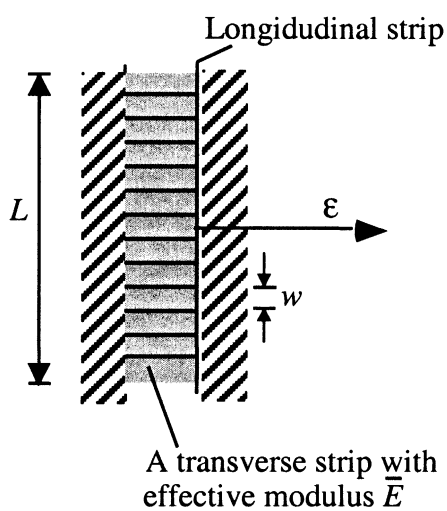

Fig. 6. A model depicting the uniform nominal in-plane deformation of many wavy beams of oxide with random wave amplitudes. Each transverse *planar* segment represents a wavy beam with a given wave amplitude, and hence the segment has a specific value of the effective elastic modulus, $\bar{E}$ (Eq. (12)), which is a sample of the random variable $\bar{E}$.

strate. The strip consists of a series of transverse segments, each representing one equivalent planar film with a given $\bar{E}$. The width, w, of each segment is small compared to the total length, L, of the longitudinal strip so that it contains a large number of segments with all possible values of $\bar{E}$. Each segment is strained by an equal amount ε along the transverse direction. The corresponding stress, $\sigma = \varepsilon\bar{E}$, is different for different segments. The mean stress is given by

$$\langle\sigma\rangle = \varepsilon\langle\bar{E}\rangle \tag{13}$$

where $\langle\rangle$ denotes the mean or the expected value. $\langle\bar{E}\rangle$ can be estimated using the theory of random vibrations [10].

Let the waviness of the oxide layer be represented by a zero mean stationary random process given by

$$z = C\sin(\omega x) + D\cos(\omega x) \tag{14}$$

where z is the height of the surface from the mean, x is the distance along the surface (for example the distance along an AFM scan line), C and D are zero mean uncorrelated Gaussian random variables with variance

$$S^2 = S_C^2 = S_D^2 \tag{15}$$

to be determined from the power spectral density (PSD) of the AFM scan. A single value ω is chosen to represent the frequency of surface waves since, as shown in Fig. 5, the effective elastic modulus of the oxide layer is nearly independent of the wavelength of the beam. The variance at any value of x of a stationary random process with a continuous range of frequencies (instead of a single frequency) is given by the integral of its PSD [10]. The integral is also denoted by the square of RMS, the root mean square. Since we have chosen a single frequency to represent the surface roughness with random variables C and D, it can be shown that [10]

$$S^2 = S_C^2 = S_D^2 = RMS^2 \tag{16}$$

where the *RMS* is determined from the AFM scan of the surface (Fig. 3). Eq. (14) can also be written as

$$z = \sqrt{C^2 + D^2}\sin(\omega x + \phi) \tag{17}$$

where ϕ is the phase angle with a uniform probability density function in the range $(0,2\pi)$, and the amplitude, $h = \sqrt{C^2 + D^2}$, of the wave has a Rayleigh probability density function [11],

$$g(h) = \frac{h}{S^2}\exp\left(-\frac{h^2}{2S^2}\right), h \geq 0 \tag{18}$$

The mean value of $\bar{E}$ is then given by

$$\langle\bar{E}\rangle = \int_0^\infty g(h)\bar{E}(h)dh \tag{19}$$

where $\bar{E}(h) \approx \bar{E}(h,d)$ for the values of the wave period, d, of interest (Fig. 5), and is given by Eq. (12) in terms of elliptic integrals.

6. Comparison between model predictions and experiments

To estimate the composite E_{comp}, S in Eq. (18) must be determined independently for the top and the bottom surfaces of the Al tensile specimen. From the AFM scans of the two surfaces and the corresponding PSDs, S_{top}=6 *nm* and S_{bottom}=3.5 *nm*. AFM data also show that $d \approx 30\ t$. Thus, for values of $t_{ox\text{-}top}$=$t_{ox\text{-}bottom}$=5 *nm*, E_{ox}=370 *GPa*, and d=30 t we obtain $\bar{E}_{ox-top} = 52.7GPa, \bar{E}_{ox-bottom} = 101.1GPa$ from Eqs. (12) and (19), and with t_{Al}=190 *nm*, E_{Al}=69 *GPa*,

$$E_{comp} = \frac{\bar{E}_{ox\text{-}top}\, t_{ox\text{-}top} + \bar{E}_{ox\text{-}bottom}\, t_{ox\text{-}bottom} + E_{Al}\, t_{Al}}{t_{ox\text{-}top} + t_{ox\text{-}bottom} + t_{Al}} = 73.2Gpa \tag{20}$$

close to the experimentally obtained E_{comp}=74.6 *GPa*.

7. Conclusion

In this work, the role of native oxide layer on the elastic modulus of Al thin films is investigated. A uniaxial tensile experiment on a 200 *nm* free-standing Al film using a MEMS sensor shows that, with the native oxide, the elastic modulus of the Al film E=74.6 *GPa*, 14% lower than the estimate using a simple composite model. An AFM scan of the film surface reveals that the native oxide is not

planar but wavy, with amplitude on the same order as the thickness of the native oxide. An analytical model is developed to determine the effective stiffness of a wavy elastic film. The model predicts that, if the wave amplitude is on the order of the film thickness, the effective elastic modulus of the wavy oxide film is only about 10% of the intrinsic modulus of the oxide. When applied to the Al-Al_2O_3 composite thin film, and when the stochastic nature of the surface is considered, the composite elastic modulus is found to be 73.2 *GPa*, close to 74.6 *GPa* determined experimentally. Therefore, in the presence of surface roughness, the stiffening effect of the oxide layer on elastic modulus is reduced. When the roughness is on the same order as the thickness of oxide layer, the stiffening effect is negligible.

Acknowledgements

SZ and KJH would like to acknowledge financial support from the NSF Grant No. CMS98-72306. TS acknowledges the support from the NSF grant ECS 97-34368. The MEMS sensor stage and the sample were fabricated in the MMS laboratory of the Department of Mechanical and Industrial Engineering, University of Illinois at Urbana Champaign (UIUC). The in-situ tensile experiments were conducted in the Environmental SEM at the Imaging Technology Group (ITG) laboratory of Beckman Institute at UIUC.

References

[1] Wafers K, Misra C. Oxides and Hydroxides of Aluminum. Alcoa Technical Report No. 19, Revised, Alcoa Laboratories, 1987, 64.
[2] Hatch John E, editor. Aluminum—Properties and Physical Metallurgy. Metal Parks, Ohio: American Society for Metals. 1984, 17.
[3] Mearini GT, Hoffman RW. J Elect Mater 1993;22(6) p. 623.
[4] Saif MTA, MacDonald NC. J MEMS 1996;5(2) p. 79.
[5] Callister Jr WD. Materials science and engineering—an introduction, 3rd ed. New York: John Wiley and Sons, 1994 p. 767.
[6] Huang H, Spaepen F. Acta Mater 2000;48(12) p. 3261.
[7] Haque MA, Saif MTA. Experimental Mechanics (in press).
[8] Haque MA, Saif MTA. Sensors and Actuators A (in press).
[9] Boresi AP, Sidebottom OM, Seely FB, Smith JO. Advanced mechanics of materials, 3rd ed. New York: John Wiley and Sons, 1978 p. 168.
[10] Crandall SH, Mark WD. Random vibration in mechanical systems. Academic Press, 1963 p. 28.
[11] Crandall SH. Mechanical properties of response to random vibration. In: Crandall SH, editor. Random vibration. Technology Press, MIT and John Wiley and Sons Inc.; 1958. p. 8-.